The effect of mixed alkali on EPR and optical absorption spectra in mixed alkali borate $x\mathrm{Na_2O}$–$(30-x)\mathrm{K_2O}$–$70\mathrm{B_2O_3}$ glasses doped with iron ions

R.P. Sreekanth Chakradhar [a,*], K.P. Ramesh [a], J.L. Rao [b], J. Ramakrishna [a]

[a] *Department of Physics, Indian Institute of Science, Bangalore 560 012, India*
[b] *Department of Physics, S.V. University, Tirupati 517 502, India*

Abstract

Electron paramagnetic resonance (EPR) and optical absorption studies of iron doped mixed alkali borate glasses, $x\mathrm{Na_2O}$–$(30-x)\mathrm{K_2O}$–$70\mathrm{B_2O_3}$ ($5 \leqslant x \leqslant 25$) have been investigated as a function of alkali content to look for the 'mixed alkali effect' on the spectral properties of the glasses. The EPR spectra of all the investigated samples exhibit resonance signals which are characteristic of the Fe^{3+} ions. The EPR spectrum exhibits an intense resonance signal at $g = 4.02 \pm 0.1$, a moderately intense signal at $g = 2.02 \pm 0.1$ and a shoulder in the region of $g = 7.20 \pm 0.5$. The existence of the resonances at $g = 4.02$ and $g = 7.20$ have been attributed to Fe^{3+} ions in rhombic and axial symmetry sites respectively. The $g = 2.02$ resonance is due to Fe^{3+} ions coupled by exchange interactions. The number of spins (N) participating in resonance and its paramagnetic susceptibility (χ) have been evaluated. It is observed that N and χ decrease with x up to $x = 10$ and then increase up to $x = 15$ exhibiting a minimum at $x = 10$ and a maximum at $x = 15$ and thereafter it gradually decreases. The optical absorption spectrum exhibits three bands assigned to $^6A_{1g}(S) \rightarrow {}^4A_{1g}(G)$, $^4E_g(G)$; $^6A_{1g}(S) \rightarrow {}^4T_{2g}(G)$ of Fe^{3+} and the other band is assigned to Fe^{2+}–Fe^{3+} inter-valence charge transfer band. From ultraviolet absorption edges, the optical bandgap and Urbach energies have been evaluated. The optical band gap energy obtained in the present work varies 2.74–3.77 eV for both the direct and indirect transitions. The physical parameters of all the glasses have been evaluated with respect to x.

PACS: 61.43.Fs; 33.35.+r; 32.30.Jc

1. Introduction

The 'mixed alkali effect' (MAE) is one of the classic 'anomolies' of glass science [1–5]. In general, most of the properties of the glass change linearly with composition. However, adding a second alkali ion to a glass changes many of its properties in a nonlinear way and it exhibits a minimum or maximum [1]. This is known as the mixed alkali effect, and has been seen in many properties including viscosity, chemical durability, alkali diffusion, electrical conductivity, and mechanical relaxation. However, the mixed alkali effect is not much studied in borate glasses. Also, reports on spectroscopic studies are very few but they would be important and useful to gain insight into the microscopic mechanisms responsible for the effect.

Electron paramagnetic resonance (EPR) and optical absorption studies are two important and useful techniques in understanding the microscopic properties in glasses. The Fe^{3+} ions are among the most thoroughly studied probes in glasses, their EPR spectra being

* Corresponding author. Tel.: +91 80 22932722; fax: +91 80 23602602.
E-mail address: chakra72@physics.iisc.ernet.in (R.P. Sreekanth Chakradhar).

typified by resonance lines at $g \approx 4.3$ and 2.0 that arise from the isotropic transitions within the Kramers doublets [6–11]. Changes in the chemical composition of glass may change the local environment of the transition metal ion incorporated into the glass, leading to ligand field changes which may be reflected in the optical absorption and EPR spectra.

The effect of mixed alkalis on the optical absorption spectra has been studied for copper and nickel ions in silicate glasses [12–14]. Ahmed et al. [15] have found only a small deviation from the linearity in the optical absorption spectral characteristics of Cu^{2+} in a couple of mixed alkali borates, with the composition of the alkali elements. However, a systematic study of the spectral characteristics in mixed alkali borate glasses is necessary to evolve a consistent understanding of the mixed alkali effect in borate glasses, as borate glasses undergo interesting structural changes with alkali content. In the present investigations we have studied sodium potassium borate glasses (hereafter, to be referred as NaKB) doped with iron ions using EPR and optical absorption techniques and the results obtained from these studies are discussed with respect to the composition of the mixed alkali elements. The physical properties of the glasses also have been evaluated with respect to the mixed alkali content.

2. Experimental

The starting materials used for the preparation of the glasses were Analar grade M_2CO_3 (M = Na and K), H_3BO_3 and Fe_2O_3. Table 1 lists the batch composition in mol% of glasses studied in the present work. The chemicals were weighed accurately in an electronic balance and ground to fine powder and mixed thoroughly. The batches were then placed in porcelain crucibles and then melted in an electrical furnace in air at 1273 K. After heat treatment the melt was then quenched at room temperature in air by pouring it onto a polished porcelain plate and pressing it with another porcelain plate. Elemental analysis of Na and K was carried out by Flame-Photometry; Fe estimation was carried out by spectro-photometry using KSCN as a complexing agent [16]. The percentage of B_2O_3 is calculated by difference and the results are presented in Table 1. As can be seen from the table, the composition given by the chemical analyses agree well with the batch composition. The errors in the compositions range from 2% to 11% which is a common occurrence in mixed oxide systems. The glass formation was confirmed by using X-ray diffraction experiments. Polished glasses of thickness 1 mm have been used for optical measurements.

Table 1
Composition of glasses studied in the present work

Glass code	Composition by batch (mol%)			Composition by analysis (mol%)				
	Na_2O	K_2O	B_2O_3	Fe_2O_3	Na_2O	K_2O	B_2O_3	Fe_2O_3
$x = 5$	5	25	69.5	0.5	5.20	23.95	70.37	0.48
$x = 10$	10	20	69.5	0.5	10.3	18.9	70.32	0.47
$x = 15$	15	15	69.5	0.5	15.3	14.8	69.40	0.48
$x = 20$	20	10	69.5	0.5	20.7	9.20	69.65	0.45
$x = 25$	25	5	69.5	0.5	25.5	4.90	69.15	0.44

EPR spectra were recorded on an EPR spectrometer operating in the X-band frequency (≈9.200 GHz) with field modulation at 100 kHz. The magnetic field was scanned from 0 to 500 mT and the microwave power used was 5 mW. A powdered glass specimen of 100 mg was taken in a quartz tube for EPR measurements. The optical absorption spectra for the glass samples were recorded at 300 K on a UV–VIS spectrophotometer in the wavelength region 350–850 nm.

2.1. X-ray diffraction studies

The X-ray diffraction is a useful technique to detect the presence of crystals in a glassy matrix if the crystals are of dimensions greater than typically 100 nm [17]. The X-ray diffraction pattern of an amorphous material is distinctly different from that of crystalline material and consists of a few broad diffuse haloes rather than sharp rings. All the samples were tested and the results showed the absence of crystalline nature. Fig. 1 shows the typical X-ray diffraction patterns for these composi-

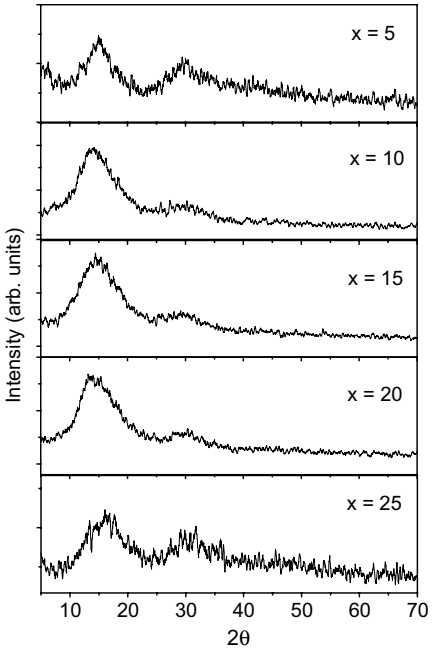

Fig. 1. X-ray diffraction pattern for different mixed alkali borate glasses – xNa_2O–$(30 - x)K_2O$–$69.5B_2O_3 + 0.5Fe_2O_3$ ($5 \leqslant x \leqslant 25$), at room temperature.

tions (see Table 1). The patterns obtained do not reveal any crystalline phase in the glass.

2.2. Physical properties of Fe^{3+} doped mixed alkali borate glasses

The density (D) of the glass samples at room temperature was measured by using Archimedes principle on a sensitive micro balance with xylene as an immersion liquid. The mean atomic volume (V) of each glass was obtained from the values of densities (D) and mean atomic weights. The number of iron ions (N) was determined from the glass composition and its density value. The refractive index (n_d) of the glass was measured with an Abbe Refractometer at a wavelength of $\lambda = 5893$ Å. The dielectric constant (ε) was calculated from the refractive index of the glass [18], using the relation

$$\varepsilon = n_d^2. \tag{1}$$

The reflection loss from the glass surface was computed from the refractive index by using the Fresnels formula as shown below [19]

$$R = \left[\frac{(n_d - 1)}{(n_d + 1)}\right]^2. \tag{2}$$

The molar refractivity (R_m) for each glass was evaluated from the following equation [20]

$$R_m = \left[\frac{(n_d - 1)}{(n_d + 2)}\right]\frac{M}{D}, \tag{3}$$

where n_d is the refractive index of refraction at $\lambda = 5893$ Å. M is the average molecular weight and D is the density in g cm^{-3}.

The electronic polarizability α_e can be calculated using the formula [21]

$$\alpha_e = \frac{3(n_d^2 - 1)}{4\pi N(n_d^2 + 2)}. \tag{4}$$

The polaron radius and inter-ionic separation can be calculated by using the formula as given by Ahmed et al. [22]

$$r_p = \frac{1}{2}\left(\frac{\pi}{6N}\right)^{1.3}, \tag{5}$$

where $\pi = 3.14$ and

$$r_i = \left(\frac{1}{N}\right)^{1/3}, \tag{6}$$

where N is the number of iron ions per unit volume.

2.3. Optical basicity of the glass (Λ_{th})

The optical basicity of an oxide glass will reflect the ability of the glass to donate negative charge to the probe ion [23]. Duffy and Ingram [24] reported that the ideal values of optical basicity can be predicted from the composition of the glass and the basicity moderating parameters of the various cations present. The theoretical values of the optical basicity of the glass can be estimated using the formula [24]

$$\Lambda_{th} = \sum_{i=1}^{n}\frac{Z_i r_i}{2\gamma_i}, \tag{7}$$

where n is the total number of cations present, Z_i is the oxidation number of the ith cation, r_i is the ratio of the number of ith cations to the number of oxides present and γ_i is the basicity moderating parameter of the ith cation. The basicity moderating parameter γ_i can be calculated [24] from the following equation:

$$\gamma_i = 1.36(x_i - 0.26), \tag{8}$$

where x_i is the Pauling electronegativity [25] of the cation. The theoretical values of optical basicity (Λ_{th}) calculated for all the glass samples (see Table 1) are listed in Table 2. This table also includes the physical parameters like densities, molar volumes, number of iron ions per unit volume, polaron radii, inter-ionic distances evaluated for the glasses studied in the present work.

Table 2
Certain physical parameters of iron doped NaKB glasses studied in the present work at room temperature (the errors in measurement are given in parenthesis)

S. no.	Physical property	Glass code				
		$x = 5$	$x = 10$	$x = 15$	$x = 20$	$x = 25$
1.	Average molecular weight (g)	83.620	82.015	80.398	78.788	77.176
2.	Density, D (g/cm^3) (±0.005)	2.587	2.552	2.734	2.598	2.600
3.	Refractive index, n_D (±0.0005)	1.5121	1.5170	1.5139	1.5110	1.5090
4.	Molar refractivity, R_M (cm^{-3}) (±0.005)	9.698	9.721	8.852	9.084	8.862
5.	Mean atomic volume, (V) (g/cm^3/atom) (±0.0002)	0.0734	0.0730	0.0668	0.0689	0.0675
6.	Optical dielectric constant, (ε) (±0.001)	2.286	2.301	2.292	2.283	2.277
7.	Electronic polarizability, $\alpha_e \times 10^{-24}$ (ions/cm^3) (±0.005)	3.843	3.852	3.507	3.599	3.512
8.	Concentration, $N \times 10^{22}$ (ions/cm^3) (±0.002)	0.932	0.937	1.024	0.993	1.015
9.	Ionic radius, r_p(Å) (±0.002)	1.915	1.911	1.856	1.875	1.861
10.	Inter-ionic distance, r_i(Å) (±0.005)	4.752	4.743	4.605	4.652	4.618
11.	Optical basicity (Λ_{th})	0.4014	0.3969	0.3924	0.3880	0.3837

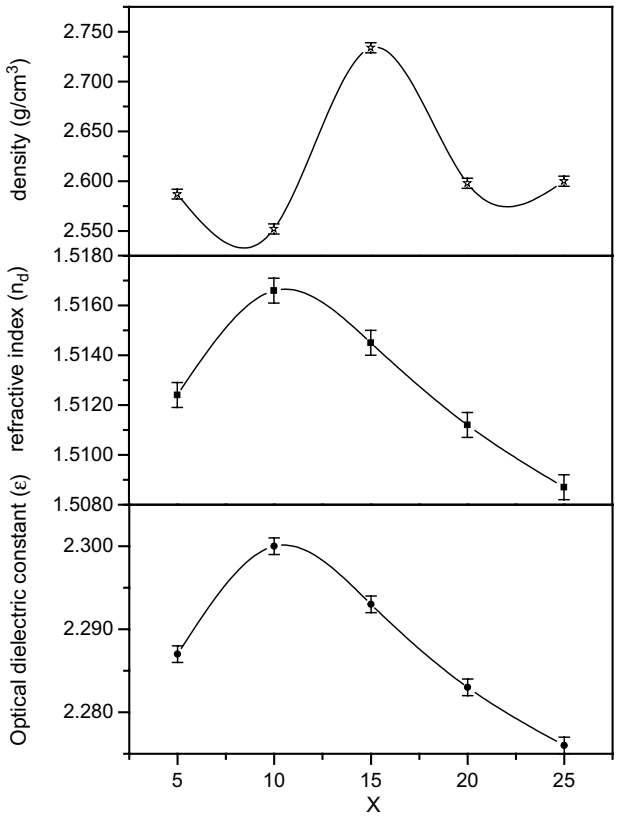

Fig. 2. Composition dependence of density, refractive index and optical dielectric constant of 0.5 mol% Fe^{3+} ions doped $x$$Na_2O$–$(30 - x)K_2O$–$70B_2O_3$ ($5 \leqslant x \leqslant 25$), at room temperature.

Fig. 2 shows the compositional dependence of density, refractive index and optical dielectric constant of the NaKB glasses at room temperature. It is observed that the density initially decreases with x up to $x = 10$ and then increases reaching a maximum at $x = 15$ and thereafter decreases. With the increase of Na_2O content (keeping the B_2O_3 content constant at 70 mol%), the number of Na atoms increases and the number of K atoms decreases. As K atoms are heavier than Na, the density should decrease continuously with increase of Na_2O content. But probably due to MAE we observe a raise in the density curve when the $x > 10$, reaching a maximum at $x = 15$ and thereafter decreases. In addition to this, the bond strengths of Na–O and K–O are different and the elastic moduli are directly influenced by the number of these bonds present in the glass sample. The refractive index and optical dielectric constant increase with x and reach a maximum around $x = 10$ and thereafter decrease showing MAE. The other parameters like molar refractivity, mean atomic volume, electronic polarizability, inter-ionic separation and ionic radius decrease with x up to $x = 15$, exhibiting a minimum and thereafter increase with x up to $x = 20$ and then decrease. However, it is observed that the average molecular weight and optical basicity of the glass decrease linearly with x as shown in Table 2.

3. Results

3.1. EPR studies

In undoped glasses no EPR signal was detected confirming that the starting materials used in the present work are free from impurities or other paramagnetic centers (defects). When the Fe^{3+} ions are introduced, the EPR spectra of all the glass samples exhibit resonance signals which are characteristic of Fe^{3+} ions. Fig. 3 shows the room temperature X-band EPR spectra of 0.5 mol% of Fe^{3+} ions in $x$$Na_2O$–$(30 - x)K_2O$–$70B_2O_3$ ($5 \leqslant x \leqslant 25$) glasses. The EPR spectrum exhibits an intense sharp resonance signal at $g = 4.02 \pm 0.1$, a moderately intense signal at $g = 2.02 \pm 0.1$ and a shoulder in the region of $g = 7.20 \pm 0.5$ for all the glass samples under investigation. It is interesting to observe that the EPR spectra exhibit a marked change, if one alkali gradually replaces the other.

3.2. Calculation of the number of spins participating in resonance

The number of spins participating in resonance can be calculated by comparing the area under the absorption curve with that of a standard ($CuSO_4 \cdot 5H_2O$ in this study) of known concentration. Weil et al. [26] gave the following expression which includes the experimental parameters of both sample and standard.

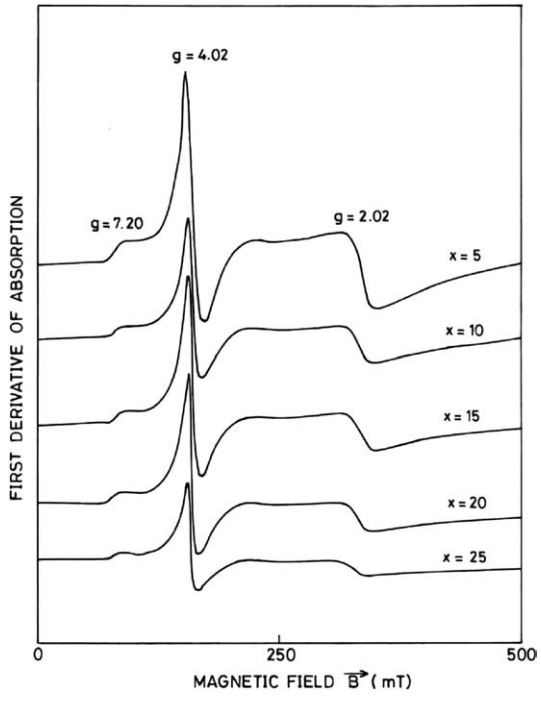

Fig. 3. EPR spectra of 0.5 mol% Fe^{3+} ions doped in different mixed alkali borate glasses – $x$$Na_2O$–$(30 - x)K_2O$–$70B_2O_3$ ($5 \leqslant x \leqslant 25$), at room temperature.

$$N = \frac{A_x(\mathrm{Scan}_x)^2 G_{\mathrm{std}}(B_{\mathrm{m}})_{\mathrm{std}}(g_{\mathrm{std}})^2[S(S+1)]_{\mathrm{std}}(P_{\mathrm{std}})^{1/2}}{A_{\mathrm{std}}(\mathrm{Scan}_{\mathrm{std}})^2 G_x(B_{\mathrm{m}})_x(g_x)^2[S(S+1)]_x(P_x)^{1/2}}\ [\mathrm{Std}], \tag{9}$$

where A is the area under the absorption curve which can be obtained by double integrating the first derivative EPR absorption curve, scan is the magnetic field corresponding to unit length of the chart, G is the gain, B_{m} is the modulation field width, g is the g factor, S is the spin of the system in its ground state. P is the microwave power. The subscripts 'x' and 'std' represent the corresponding quantities for Cu^{2+} glass sample and the reference ($CuSO_4 \cdot 5H_2O$) respectively. The composition dependence of the number of spins participating in resonance for Fe^{3+} ions in NaKB glasses at room temperature for the signals at $g = 4.02$ and $g = 2.02$ are shown in Fig. 4. It is observed that, initially N decreases with x up to $x = 10$ and then increases up to $x = 15$ exhibiting a minimum at $x = 10$ and a maximum at $x = 15$ and thereafter it gradually decreases.

3.3. Calculation of the paramagnetic susceptibility (χ) from EPR data

The EPR data can be used to calculate the paramagnetic susceptibility of the sample using the formula [27]

$$\chi = \frac{Ng^2\beta^2 J(J+1)}{3k_{\mathrm{B}}T}, \tag{10}$$

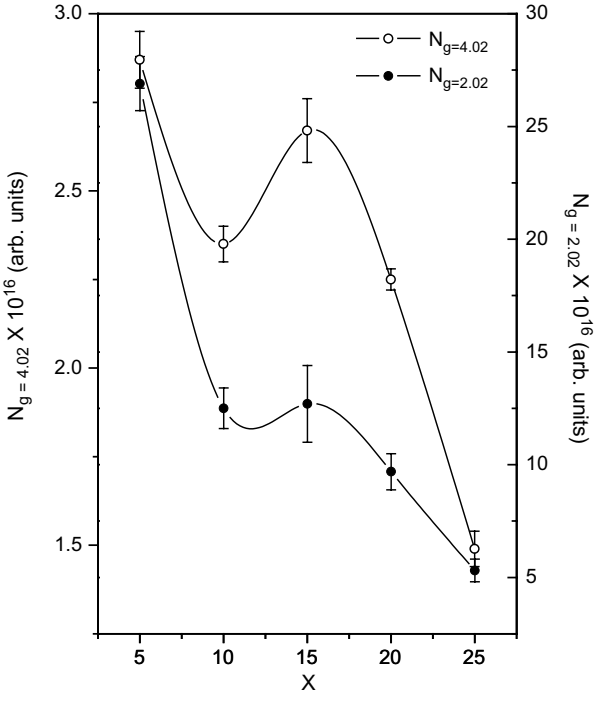

Fig. 4. The variation of number of spins for $g = 4.02$ ($N_{g=4.02}$) and $g = 2.02$ ($N_{g=2.02}$) resonances with x in different mixed alkali borate glasses $x\mathrm{Na_2O}$–$(30 - x)\mathrm{K_2O}$–$69.5\mathrm{B_2O_3} + 0.5\mathrm{Fe_2O_3}$ ($5 \leqslant x \leqslant 25$), at room temperature.

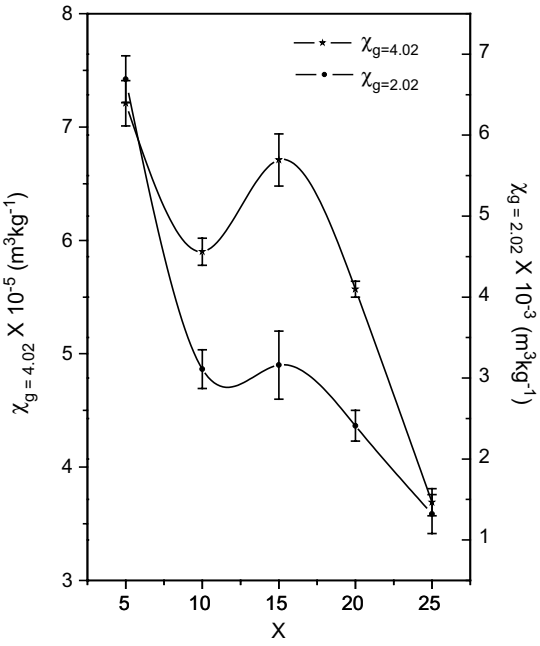

Fig. 5. The variation of paramagnetic susceptibility (χ) for $g = 4.02$ ($N_{g=4.02}$) and $g = 2.02$ ($N_{g=2.02}$) resonances with x in different mixed alkali borate glasses $x\mathrm{Na_2O}$–$(30 - x)\mathrm{K_2O}$–$69.5\mathrm{B_2O_3} + 0.5\mathrm{Fe_2O_3}$ ($5 \leqslant x \leqslant 25$), at room temperature.

where N is the number of spins per m^3 and the other symbols have their usual meaning. N can be calculated from Eq. (9) and g is taken from EPR data. It is observed that the paramagnetic susceptibility decreases with x up to $x = 10$ and then increases up to $x = 15$ and thereafter it gradually decreases as shown in Fig. 5.

3.4. Optical absorption studies

Fig. 6 shows the optical absorption spectra observed in the glasses, studied in the present work. The observed bands are characteristic of both Fe^{3+} and Fe^{2+} ions in octahedral coordination. The observed bands are assigned as follows: $^6A_{1g}(S) \rightarrow {}^4A_{1g}(G)$, $^4E_g(G) \sim 450$ nm (22216 cm^{-1}); $^6A_{1g}(S) \rightarrow {}^4T_{2g}(G) \sim 557$ nm (17948 cm^{-1}); features as ascribed to the deviations of the iron site from ideal octahedral symmetry.

3.5. Optical band gaps

The study of the fundamental absorption edge in the UV-region is a useful method for the investigation of optical transitions and electronic band structure in crystalline and non-crystalline materials. There are two types of optical transitions, which can occur at the fundamental absorption edge of crystalline and non-crystalline semiconductors. They are direct and indirect transitions. In both the cases, electromagnetic waves interact with the electrons in the valence band, which are raised across the fundamental gap to the conduction

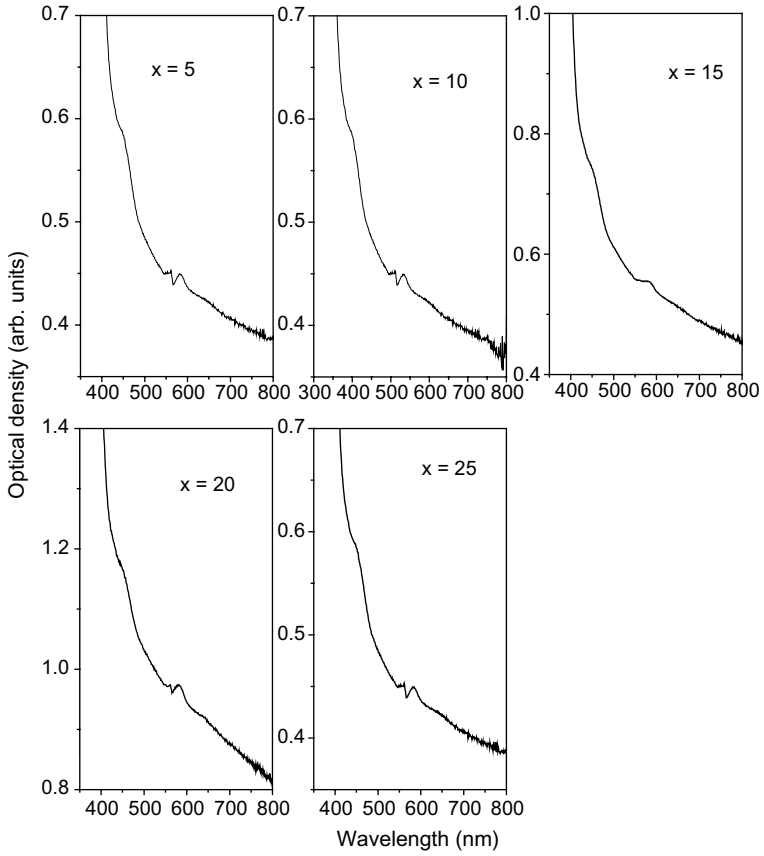

Fig. 6. Optical absorption spectra of different mixed alkali borate glasses – xNa$_2$O–(30 – x)K$_2$O–69.5B$_2$O$_3$ + 0.5Fe$_2$O$_3$ ($5 \leqslant x \leqslant 25$), at room temperature.

band. In glasses, the conduction band is influenced by the glass forming anions; the cations play an indirect but significant role [28,29]. The Urbach energy gives the width of the tails of localized states within the optical band gap. At the absorption edge, random internal electric fields will dominate the broadening of the excitation levels due to the lack of long-range order or presence of defects [28,30]. The least ΔE, i.e., sharp absorption edge, suggests that defects are the minimum facilitating long-range order.

A main feature of absorption edge of amorphous semiconductors, particularly at the lower values of absorption coefficient, is the exponential increase of the absorption coefficient $\alpha(v)$ with photon energy hv in accordance with an empirical relation [31]

$$\alpha(v) = \alpha_0 \exp\left(\frac{hv}{\Delta E}\right), \tag{11}$$

where α_0 is a constant, ΔE is the Urbach energy and v is the frequency of radiation.

The absorption coefficient $\alpha(v)$ can be determined near the edge using the formula:

$$\alpha(v) = \left(\frac{1}{d}\right) \ln\left(\frac{I_0}{I}\right) = 2.303\frac{A}{d}, \tag{12}$$

where A is the absorbance at frequency v and d is the thickness of the sample. For an absorption by an indirect transition, the equation takes the form:

$$E_{\text{opt}} = hv - \left(\frac{hv}{B}\right)^{1/2}. \tag{13}$$

Using the above equations, by plotting $(\alpha hv)^{1/2}$ and $(\alpha hv)^2$ as a function of photon energy hv, one can find the optical energy band gaps (E_{opt}) for indirect and direct transitions respectively by extrapolating the linear region of the curve to the hv axis and is shown in Figs. 7 and 8 respectively. Plots were also drawn between $\ln\alpha$ and hv (not shown in the figure) and from these plots, the slopes and thereby Urbach energies have been calculated. The optical band gaps and Urbach energies obtained in the present work are given in Table 3.

4. Discussion

4.1. EPR studies

A trivalent iron ion, (Fe^{3+}), has electronic configuration $3d^5$ corresponding to a half filled d-shell and is par-

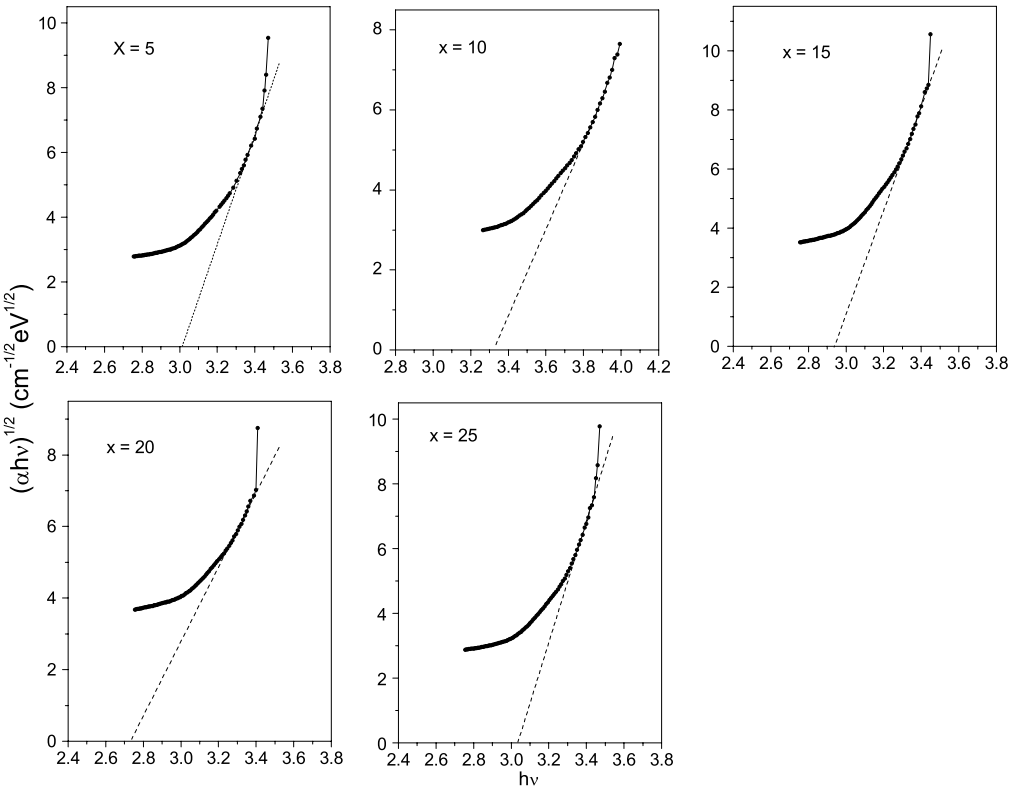

Fig. 7. Plots corresponding $(\alpha h\nu)^{1/2}$ vs $h\nu$ for different mixed alkali borate glasses – xNa$_2$O–(30 − x)K$_2$O–69.5B$_2$O$_3$ + 0.5Fe$_2$O$_3$ ($5 \leqslant x \leqslant 25$), at room temperature.

ticularly the most stable. In crystalline fields, the usual high-spin state is common (i.e., $t_{2g}^3 e_g^2$ configuration with one unpaired electron in each of the orbitals). The low spin state which is less common has the t_{2g}^5 configuration with two pairs of paired electrons and one unpaired electron. Since the iron ions in Fe^{3+} state belong to d^5 configuration with ^6S as ground state in the free ion and there is no spin–orbit interaction [11], the g value is expected to lie very near the free-ion value of 2.0023. However, a g value very much greater than 2.0 often occurs; in particular an isotropic g value of 4.02 occurs and these large g values arise when certain symmetry elements are present. The theory of these large g values is usually expressed by the spin-Hamiltonian [32]

$$H = g\beta BS + D[S_z^2 - \{S(S+1)/3\}] + E(S_x^2 - S_y^2), \qquad (14)$$

where $S = 5/2$. Here D and E are the axial and rhombic structure parameters, $\lambda = E/D$ lies within the limits $0 < \lambda < 1/3$ [33].

When Fe^{3+} impurity complexes are situated in crystal field with a large axial component, the free ion ^6S state splits into three Kramers doublets $|\pm 1/2\rangle$, $|\pm 3/2\rangle$ and $|\pm 5/2\rangle$ with separations usually greater than the microwave quantum. Normally, the selection rules permit EPR transitions in the $|\pm 1/2\rangle$ doublet with $g \approx 2.0$ and 6.0 [34,35]. In a large number of glasses and other Fe^{3+} containing materials a symmetric and isotropic line at $g \approx 4.0$–4.2 is observed. Castner et al. [6] explained it as arising from the middle Kramers doublet containing admixture of different $|\pm m_j\rangle$ states, which are caused by the presence of low symmetry term $E(S_x^2 - S_y^2)$ in the Hamiltonian.

The EPR spectra of Fe^{3+} ions in various glasses have been extensively studied [6,11,36–49]. Usually, occurrence of two resonance signals, at $g = 4.2$ and 2.0, has been reported [6,9,11]. In some cases, the resonance near $g = 6.0$ was also observed [6,9,11,45] as a shoulder of the resonance near $g = 4.2$. The resonances at $g = 4.2$ and $g = 2.0$ have been interpreted in different ways [6,9–11]. Some investigators [6,10,11] suggested that the value of g in glasses containing Fe^{3+} ions is related to the coordination number. The absorption at $g = 4.2$ and 2.0 arise from Fe^{3+} ions in tetrahedral and octahedral coordinations respectively [10].

On the other hand, Kurkjian and Sigety [9] showed that the resonance signals at $g = 4.2$ and 2.0 cannot be used as a direct indication of coordination number for Fe^{3+} ions and suggested that the $g = 4.2$ resonance signal is due to low symmetry (rhombic) sites of either tetrahedral or octahedral coordination. This interpretation has been supported by Loveridge and Parke [11]. An effective g value of $g_{eff} \approx 9.7$ was also reported for Fe^{3+} ions in glasses [40,46]. According to Wickman et al. [7], Fe^{3+} in rhombic vicinities shows the transition

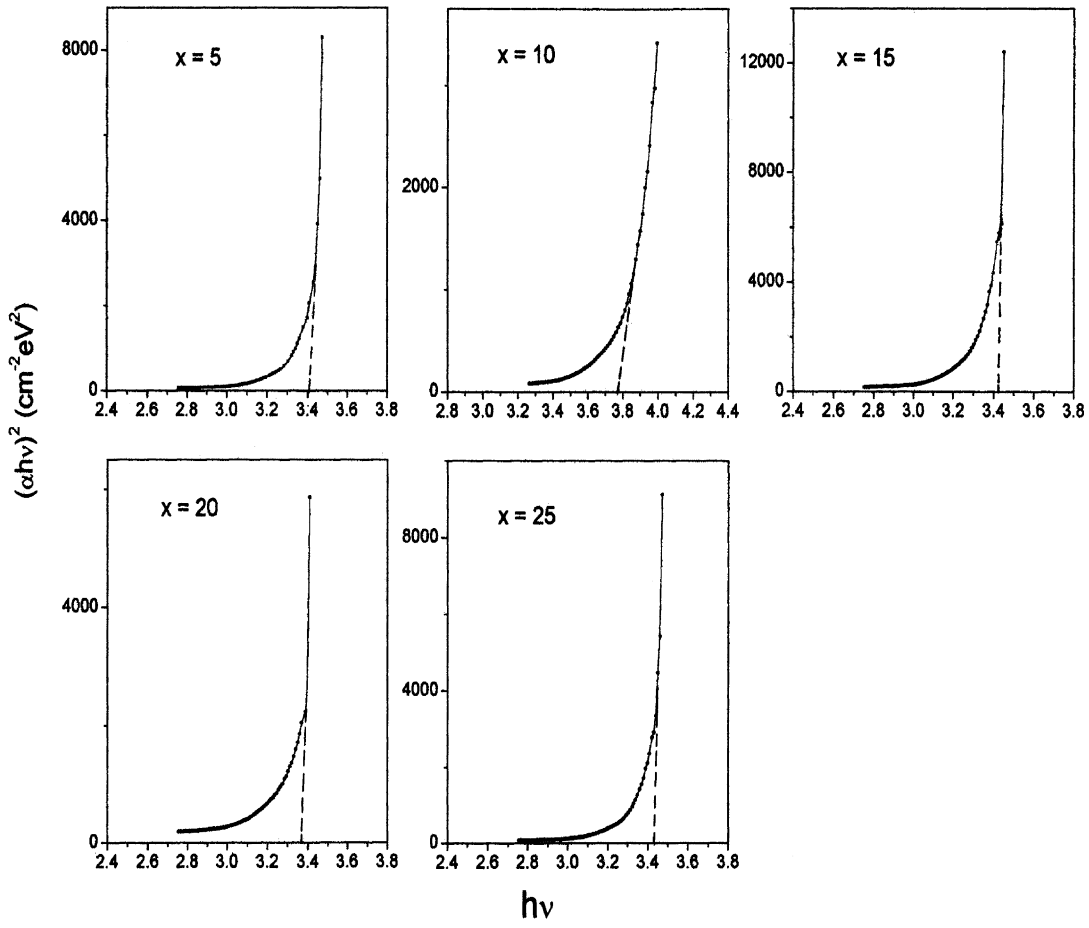

Fig. 8. Plots corresponding $(\alpha h\nu)^2$ vs $h\nu$ for different mixed alkali borate glasses – xNa$_2$O–(30 − x)K$_2$O – 69.5B$_2$O$_3$ + 0.5Fe$_2$O$_3$ ($5 \leqslant x \leqslant 25$), at room temperature.

Table 3
Observed band positions, optical band gap and Urbach energies for iron ions in NaKB glass matrices with x

Glass code	Transition from $^6A_{1g}(S)\rightarrow$		Charge transfer band position (cm^{-1})	Optical Band gap		Urbach energy $\Delta E \pm 0.002$ (eV)
	$^4A_{1g}(G)$, $^4E_g(G)$ (cm^{-1})	$^4T_{2g}(G)$ (cm^{-1})		Indirect ± 0.04 (eV)	Direct ± 0.04 (eV)	
$x = 5$	22216	17948	17089	3.01	3.40	0.277
$x = 10$	24684	19564	18756	3.32	3.77	0.357
$x = 15$	22166	–	17147	2.95	3.41	0.250
$x = 20$	22117	17852	17147	2.74	3.38	0.294
$x = 25$	22116	17852	17147	3.04	3.43	0.238

having $g \approx 4.2$ isotropic value corresponding to median Kramers doublet, and other transitions corresponding to the other two doublets characterized by g factors (9.678; 0.857; 0.607) having a pronounced anisotropy. These transitions result in a large background with effective g values from 1 to 10 as pointed out by Griffith [50].

In the present work, the existence of the resonance signals at $g = 4.02$ and $g = 7.20$ have been attributed to Fe^{3+} ions in rhombic and axial symmetry sites respectively, whereas the $g = 2.02$ resonance is due to Fe^{3+} ions coupled by exchange interactions. The g values have been calculated as a function of x in NaKB glasses, and it is found that the g values do not vary much with x and are the same within the error of measurement in all the samples. These g values indicate that the paramagnetic ion is in the trivalent state and the site symmetry is distorted octahedral. This independent behavior of g values with composition of glass allows us to conclude that the symmetry around the paramagnetic Fe^{3+} ions is independent of alkali ions present in the samples. It is also observed that the peak-to-peak widths (ΔB_{pp}) of the resonance line at $g = 4.02 \pm 0.1$ and 2.02 ± 0.1 are found to be independent of x. In the present work we have observed a peak-to-peak width of approximately

10.8 mT for $g \approx 4.02$ and 40.8 mT for $g \approx 2.0$ resonance lines respectively. The peak-to-peak width obtained in the present work is comparable to those obtained for Fe^{3+} ions in lead borotellurite (12.5 mT for $g \approx 4.2$ resonance line) glasses reported by Ardelean et al. [46].

Analyzing the number of Fe^{3+} ions participating in the resonance it is observed that, initially it decreases with x up to $x = 10$ and then increases up to $x = 15$ exhibiting a minimum at $x = 10$ and a maximum at $x = 15$ and thereafter it gradually decreases. This type of non-linear variation of N with x, exhibiting a minimum and maximum may be attributed to the MAE and may be due to the conversion of Fe^{3+} to Fe^{2+} with x. The Fe^{2+} ions are not involved in the EPR absorption but their interaction with Fe^{3+} may influence the characteristics of the EPR absorption lines. The optical absorption spectrum supports the simultaneous presence of both Fe^{3+} and Fe^{2+}.

From Fig. 5 we can observe that the paramagnetic susceptibility decreases with x up to $x = 10$ and then increases up to $x = 15$ and thereafter it gradually decreases. These changes may be due to the same reasons viz., MAE and conversion of Fe^{3+} to Fe^{2+} with x as discussed earlier.

4.2. Optical absorption studies

Among all transition metal ions, Fe^{3+} (d^5 configuration) ion is of special interest because it is the only configuration for which there are no spin-allowed transitions possible and only weak bands may occur corresponding to spin-forbidden transitions. The 3d transition metal ions are in octahedral or tetrahedral symmetry with their nearest neighbor anions. Their free energy levels for octahedral or tetrahedral coordination split by the action of ligand field. The optical absorption spectra of the glasses studied in the present work exhibits bands which are characteristic of both Fe^{3+} and Fe^{2+} ions in octahedral coordination. The observed bands are assigned as follows $^6A_{1g}(S) \rightarrow {}^4A_{1g}(G)$, $^4E_g(G) \sim 450$ nm (22 216 cm^{-1}); $^6A_{1g}(S) \rightarrow {}^4T_{2g}(G) \sim 557$ nm (17 948 cm^{-1}); features as ascribed to the deviations of the iron site from ideal octahedral symmetry. It would also be expected that the $^4T_{2g}(G)$ state would split under these site distortions [51].

The simultaneous presence of both Fe^{3+} and Fe^{2+} raises the possibility of inter-valence charge transfer electronic transitions between Fe^{2+} and Fe^{3+}. It is proposed that the ~583 nm (17 147 cm^{-1}) band, which is not directly correlated with the iron content, be assigned to Fe^{2+}–Fe^{3+} inter-valence charge transfer band. Burns [52] has examined a series of orthopyroxenes and has attributed the Fe^{2+}–Fe^{3+} inter-valence charge transfer to an absorption in the 760–800 nm regions. Such a feature similarly occurs in this region for aegirine mineral, the ferric ion end-member $NaFe(SiO_3)_2$. The question arises of why the inter-valence charge transfer band of pyroxene mineral Jadeite is at much higher energy. Burns [52] concluded that the ~780 nm charge transfer band in high iron orthopyroxenes arises from the interaction of Fe^{2+} in the large M2 position (electron transfer process), (where M2 represents cations such as Al^{3+}, Fe^{3+}, Ti^{3+} etc.) and Fe^{3+} in the distorted octahedral M1 position. This conclusion was partially based on polarization information.

Nevertheless, it is proposed by Rossman [51] that both the divalent and trivalent iron which give rise to the inter-valence charge transfer band are located in the octahedral sites. The spectroscopic evidence supports this interpretation when compared with other minerals [51] wherein inter-valence charge transfer is believed to occur between adjacent octahedral sites. The charge transfer band (inter-valence) observed in Jadeite at ~573 nm (17 447 cm^{-1}) [51] compares favorably with corundum at ~600 nm (16 665 cm^{-1}) [52], kyanite at ~590 nm (16 945 cm^{-1}) [53] and cordierite at ~571 nm (17 508 cm^{-1}) [54]. Therefore, in the present investigations the presence of a band at ~583 nm (17 147 cm^{-1}) is attributed to the Fe^{2+}–Fe^{3+} inter-valence charge transfer band. This band is observed in all the glasses. However, the band corresponding to the transition $^6A_{1g}(S) \rightarrow {}^4T_{2g}(G)$ is obscured by an intense valence charge transfer band when the two alkali contents are equal (i.e., $x = 15$) It is also observed that the band positions of $x = 10$ glass shifts slightly towards higher energy side. The bands assigned are comparable to those found in literature [51–55].

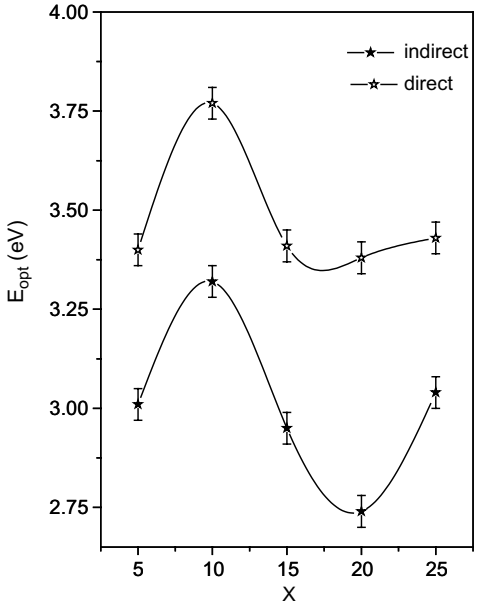

Fig. 9. Composition dependence of optical band gap energy (E_{opt}) of 0.5 mol% Fe^{3+} ions doped xNa_2O–$(30 - x)K_2O$–$70B_2O_3$ ($5 \leqslant x \leqslant 25$), at room temperature.

It is observed that in the present work the optical band gap energies vary from 2.74 to 3.77 eV for both the direct and indirect transitions (see Fig. 9), which is of the same order expected for borate glasses. It is evident from Table 3, that Urbach energy (0.238 eV) is minimum for $x = 25$ in the glass samples. This suggests that defects in these glasses are at a minimum.

5. Conclusions

The EPR spectra of all the investigated samples exhibit three resonance signals at $g = 7.20$, $g = 4.02$ and $g = 2.02$ at room temperature. The resonances at $g = 7.20$ have been attributed to Fe^{3+} ions in axial symmetry sites whereas the resonance at $g = 4.02$ due to isolated Fe^{3+} ions in rhombic symmetry site. The $g = 2.02$ resonance is due to Fe^{3+} ions coupled by exchange interaction. It is found that the g values are the same within the error of measurement in all the samples. These g values indicate that the paramagnetic ion is in trivalent state and is in distorted octahedral site symmetry. This independence of g values with composition of glass allows us to conclude that the symmetry around the paramagnetic Fe^{3+} ions is independent of composition of alkali ions present in the samples. It is also observed that the peak-to-peak widths (ΔB_{pp}) of the resonance line at $g = 4.02$ and 2.02 are found to be independent of x. The number of spins participating in resonance (N) and its paramagnetic susceptibility (χ) have been calculated for the resonance lines at $g = 4.02$ and $g = 2.02$ as a function of x. The variation of number of spins participating in resonance can be attributed to MAE besides conversion of Fe^{3+} to Fe^{2+} with x. The optical absorption spectrum also supports the simultaneous presence of both Fe^{3+} and Fe^{2+}. The optical absorption spectrum exhibits three bands assigned to $^6A_{1g}(S) \rightarrow {}^4A_{1g}(G)$, $^4E_g(G)$; $^6A_{1g}(S) \rightarrow {}^4T_{2g}(G)$ to Fe^{3+} and the other band assigned to Fe^{2+}–Fe^{3+} inter-valence charge transfer band. From the ultraviolet absorption edges the optical band gap energies have been evaluated and it varies 2.74–3.77 eV for both the direct and indirect transitions.

The existing theories of MAE have been proposed mainly on the basis of transport properties in mixed alkali glasses, particularly electrical. On the other hand, spectroscopic investigations on mixed alkali effects are very meagre and appropriate theoretical models are not available. The present investigation is a part of a programme to study MAE using spectroscopic techniques and we have shown that the EPR/optical parameters do show mixed alkali effect. Further work is needed with other spectroscopic techniques like Raman, IR etc., so that appropriate theoretical models could be developed. We hope that such studies will draw the attention of theorists.

Acknowledgments

Dr RPSC gratefully acknowledges the Science and Engineering Research Council (SERC), Department of Science and Technology (DST) New Delhi for the award of a Fast Track research project under Young scientist scheme.

References

[1] D.E. Day, J. Non-Cryst. Solids 21 (1976) 343.
[2] M.D. Ingram, Phys. Chem. Glasses 28 (1987) 215.
[3] M.D. Ingram, Glasstech. Ber. 67 (1994) 151.
[4] A. Bunde, M.D. Ingram, P. Maass, J. Non-Cryst. Solids 172–174 (1994) 1222.
[5] J.E. Shelby, Introduction to Glass Science & Technology, Royal Society of Chemistry, Cambridge, UK, 1997.
[6] T. Castner, G.S. Newell Jr., W.C. Holton, C.P. Slichter, J. Chem. Phys. 32 (1960) 668.
[7] H.H. Wickman, M.P. Klein, D.A. Shirley, J. Chem. Phys. 42 (1965) 2113.
[8] R.W. Kedzie, D.H. Lyons, N.M. Kestigian, Phys. Rev. 138 (1965) 918.
[9] C.R. Kurkjian, E.A. Sigety, Phys. Chem. Glasses 9 (1968) 73.
[10] C. Hirayama, J.G. Castle Jr., M. Kuriyama, Phys. Chem. Glasses 9 (1968) 109.
[11] D. Loveridge, S. Parke, Phys. Chem. Glasses 12 (1971) 90.
[12] W.H. Turner, J.A. Turner, J. Am. Ceram. Soc. 55 (1972) 201.
[13] S. Sakka, K. Kamiya, H. Yoshikawa, J. Non-Cryst. Solids 27 (1978) 289.
[14] H. Hosono, H. Kawazoe, T. Kanazawa, Yogyo-kyokai-shi 86 (1978) 567.
[15] A.A. Ahmed, A.F. Abbas, F.A. Moustafa, Phys. Chem. Glasses 24 (1983) 43.
[16] J. Mendam, R.C. Denney, J.D. Barnes, M. Thomas, Vogel's – Text Book of Quantitative Chemical Analysis, 6th Ed., Pearson Education, Singapore, 2004, p. 658.
[17] G.W. Anderson, W.D. Luehrs, J. Appl. Phys. 39 (1969) 1634.
[18] B. Bendow, P.K. Benerjee, M.G. Drexhage, J. Lucas, J. Am. Ceram. Soc. 65 (1985) C92.
[19] Y. Ohisti, S. Mitachi, T. Tanabe, Phys. Chem. Glasses 24 (1983) 135.
[20] J.E. Shelby, J. Ruller, Phys. Chem. Glasses 28 (1987) 262.
[21] A. Klinokowski, J. Non-Cryst. Solids 72 (1985) 117.
[22] M.M. Ahmed, C.A. Hogarth, M.N. Khan, J. Mater. Sci. Lett. 19 (1984) 4040.
[23] E. Guedes de Sousa, S.K. Mendiratta, J.M. Machado da Silva, Portugal. Phys. 17 (1986) 203.
[24] J.A. Duffy, M.D. Ingram, J. Inorg. Nucl. Chem. 37 (1975) 1203.
[25] L. Pauling, The Nature of Chemical Bond, 3rd Ed., Cornell University, New York, 1960, p. 93.
[26] J.A. Weil, J.R. Bolton, J.E. Wertz, Electron Paramagnetic Resonance-elementary Theory and Practical Applications, Wiley, New York, 1994, p. 498.
[27] N.W. Aschcroft, N.D. Mermin, Solid State Physics, Harcourt College Publishers, 2001, p. 656.
[28] Gan Fuxi, Optical and Spectroscopic Properties of Glass, Springer, Berlin, 1992, p. 62.
[29] P. Nachimuthu, P. Harikrishnan, R. Jagannathan, Phys. Chem. Glasses (1996) 59, and references there in.
[30] E.A. Davis, N.F. Mott, Phil. Mag. 22 (1970) 903.
[31] M.A. Hassan, C.A. Hogarth, J. Mater. Sci. 23 (1988) 2500.
[32] B. Bleaney, K.W.H. Stevens, Rep. Prog. Phys. 16 (1953) 108.
[33] J.H. Van Vleck, W.G. Penny, Phil. Mag. 17 (1934) 961.

[34] A. Abragam, B. Bleaney, Electron Paramagnetic Resonance of Transition Ions, Clarendon, Oxford, 1970, p. 203.
[35] J.R. Pilbrow, Transition Ion Electron Paramagnetic Resonance, Clarendon, Oxford, 1990, p. 135.
[36] N. Iwamoto, Y. Mokino, S. Kasahara, J. Non-Cryst. Solids 55 (1983) 113.
[37] M.L. Baesso, E.C. da silva, F.C.G. Gandra, H. Vargas, P.P. de Abreu, Filho, F. Galembeck, Phys. Chem. Glasses 31 (1990) 122.
[38] K. Tanaka, K. Kamiya, T. Yoko, S. Tanabe, K. Hirao, N. Soga, Phys. Chem. Glasses 32 (1991) 16.
[39] R.V. Anavekar, N. Devaraj, K.P. Ramesh, J. Ramakrishna, Phys. Chem. Glasses 33 (1992) 116.
[40] C. Legin, J.Y. Buzare, C. Jacoboni, J. Non-Cryst. Solids 161 (1993) 112.
[41] N.A. Eissa, W.M. El-Meliegy, S.M. El-Minyawi, N.H. Sheta, H.A. Sallam, Phys. Chem. Glasses 34 (1993) 31.
[42] E.M. Yahiaoui, R. Berger, T. Servant, J. Kliava, L. Cugunov, A. Mednir, J. Phys.: Condens. Mater. 6 (1994) 9415.
[43] R. Berger, J. Kliava, E.M. Yahiaoui, J.C. Bissey, P.K. Zinsou, P. Beziade, J. Non-Cryst. Solids 180 (1995) 151.
[44] A.S. Rao, R.R. Reddy, T.V.R. Rao, J.L. Rao, Solid State Commun. 96 (1995) 701.
[45] J. Lakshmana Rao, A. Murali, E. Dhananjaya Rao, J. Non-Cryst. Solids 202 (1996) 215.
[46] I. Ardelean, M. Peteanu, S. Flip, V. Simon, G. Gyorffy, Solid State Commun. 102 (1997) 341.
[47] C. Prakash, S. Husain, R.J. Singh, S. Mollah, J. Alloys Compd. 326 (2001) 47.
[48] I. Ardelean, M. Peteanu, V. Simon, F. Ciorcas, V. Ioncu, J. Mater. Sci. Lett. 20 (2001) 947.
[49] P. Giri Prakash, A. Murali, J.L. Rao, Phys. Chem. Glasses 43 (2002) 102.
[50] J.S. Griffith, Molec. Phys. 8 (1964) 213.
[51] G.R. Rossman, Am. Mineral. 59 (1974) 868.
[52] R.G. Burns, Mineralogical Applications of Crystal Field Theory, Cambridge University, 1970, p. 87.
[53] G.H. Faye, Am. Mineral. 56 (1971) 344.
[54] G.H. Faye, E.H. Nickel, Can. Mineral. 10 (1969) 35.
[55] G.H. Faye, P.G. Manning, E.H. Nickel, Am. Mineral. 53 (1968) 1174.